

Physiological and Metabolic Responses for Hexadecane Degradation in *Acinetobacter oleivorans* DR1

Jaejoon Jung, Jaemin Noh, and Woojun Park*

Division of Environmental Science and Ecological Engineering, Korea University, Seoul 136-713, Republic of Korea

(Received September 29, 2010 / Accepted December 10, 2010)

The hexadecane degradation of *Acinetobacter oleivorans* DR1 was evaluated with changes in temperature and ionic salt contents. Hexadecane degradation of strain DR1 was reduced markedly by the presence of sodium chloride (but not potassium chloride). High temperature (37°C) was also shown to inhibit the motility, biofilm formation, and hexadecane biodegradation. The biofilm formation of strain DR1 on the oil-water interface might prove to be a critical physiological feature for the degradation of hexadecane. The positive relationship between biofilm formation and hexadecane degradation could be observed at 30°C, but not at low temperatures (25°C). Alterations in cell hydrophobicity and EPS production by temperature and salts were not correlated with biofilm formation and hexadecane degradation. Our proteomic analyses have demonstrated that metabolic changes through the glyoxylate pathway are important for efficient degradation of hexadecane. Proteins involved in fatty acid metabolism, gluconeogenesis, and oxidative stress defense proteins appear to be highly expressed during biodegradation of hexadecane. These results suggested that biofilm formation and oxidative stress defense are important physiological responses for hexadecane degradation along with metabolic switch to glyoxylate pathway in strain DR1.

Keywords: *Acinetobacter*, biofilm, hydrocarbon degradation, motility, proteomic analysis

Many hydrocarbon-utilizing bacteria form biofilms on the oil-water interface to overcome the low water solubility of hydrocarbon and gain access to it. In such cases, the biofilm is where bacterial degradation primarily takes place. It has been demonstrated that *Acinetobacter venetianus* VE-C3 forms cell aggregates and adheres to a mixture of C₁₂ to C₂₈ *n*-alkane (Baldi *et al.*, 1999). This adhesion may help nanometer-sized *n*-alkane droplets incorporate into a thick polysaccharide biofilm matrix, and its consequent utilization by cells. The marine hydrocarbonoclastic bacterium *Alcanivorax borkumensis* also forms biofilms on hydrocarbon surfaces and its genome harbors putatively biofilm-related genes, such as those associated with exopolysaccharide metabolism, alginate biosynthesis, Type II secretion system, and Type IV pili (Schneiker *et al.*, 2006).

Many studies have noted that cellular appendages such as flagella and flagella-mediated motility perform a pivotal role in biofilm formation. In *Pseudomonas aeruginosa* biofilm, the type IV pili-defective mutant failed to develop microcolonies after monolayer attachment to a PVC surface and non-motile *flgK* mutant cells rarely attached to the same surface, suggesting that flagellar motility performs an indispensable function in initial cell-to-surface interaction and biofilm maturation processes (O'Toole and Kolter, 2006). Cell hydrophobicity has also been suggested as a factor affecting the initial attachment of cells to surfaces (van Loosdrecht *et al.*, 1990). In general, hydrophobic cells tend to attach to hydrophobic surfaces such as polystyrene surfaces (Pompilio *et al.*, 2008). Additionally, hydrocarbon degradation requires bacterial cells to adapt

their metabolic pathways as well. The proteomic analysis data strongly indicates that alkane degradation induces a variety of alkane terminal oxidation systems and modifies metabolic and physiological activities, including intracellular carbon fluxes and membrane lipid composition (Sabirova *et al.*, 2006).

Recently, a novel diesel-degrading *Acinetobacter oleivorans* DR1 has been isolated and its genome has been completely sequenced (Jung and Park, 2010; Kang *et al.*, 2010). Genome analysis revealed that genes required for degradation of a variety of hydrocarbons and aromatic compounds are present in DR1 genome, suggesting important role of this strain in bioremediation. In this study we attempted to evaluate biofilm formation, which may perform a significant function in hydrocarbon degradation and its related physiology in strain DR1 during hexadecane degradation. The metabolic adaptation induced by hexadecane utilization was evaluated via proteomic analysis.

Materials and Methods

Bacterial strains and culture conditions

Acinetobacter oleivorans DR1 (Jung and Park, 2010; Kang and Park, 2010a, 2010b, 2010c) was routinely cultured in nutrient broth (NB) with shaking at 220 rpm at 30°C. Minimal salt basal medium (MSB) (Stanier *et al.*, 1966) was employed as a minimal medium when a sole carbon source was provided. Sodium chloride and potassium chloride were used at 1% (w/v) concentration in all experiments.

Gas chromatographic analysis of hexadecane degradation

Hexadecane degradation in MSB medium supplemented with 1% (v/v) of hexadecane (Sigma, USA) was monitored via gas chromatography.

* For correspondence. E-mail: wpark@korea.ac.kr; Tel: +82-2-3290-3067; Fax: +82-2-953-0737

graphy performed on a Younglin Acme 6100 gas chromatograph equipped with an HP-5MS (Agilent, USA) capillary column and a flame ionization detector. Cells were inoculated at $\sim 10^6$ CFU/ml to 20 ml of MSB and cultured with aeration by shaking at 220 rpm. Aliquots (2 μ l) were prepared via the addition of 5 ml of dichloromethane to medium, followed by 1 min of vortexing and 15 min of centrifugation at $1,500\times g$ to separate the two phases. The oven was programmed as follows: 50°C for 3 min, raised to 300°C at 8°C/min, and an 3 min of isothermal period. The injector temperature was set to 280°C, and the detector temperature was 310°C.

Biofilm assay

Cells were washed twice in phosphate-buffered saline (PBS) and inoculated at $\sim 10^6$ CFU/ml in 200 μ l of 1/10 diluted NB and cultured in 96-well microplates for three days statically. Biofilm formation was determined by absorbance measurements at 595 nm in a 0.1% crystal violet solubilized in 95% ethanol solution, using a microtiter plate reader (PowerWaveXS, Bio-Tek, USA). Possible different growths under the testing conditions were excluded by normalizing absorbance with OD₆₀₀ (Lee *et al.*, 2008).

Motility test

Swimming and swarming motility were evaluated on 0.2% and 0.5% agar plates, respectively. Cells were grown overnight in NB medium and 2 μ l of culture was spotted onto an agar plate. Swimming and swarming were noted after 24 and 72 h of inoculation, respectively.

Microbial adherence to *n*-hexadecane (MATH) test

Cell hydrophobicity was evaluated via a MATH test (Rosenberg *et al.*, 1980). Two milliliters of bacterial suspension in distilled water at OD₆₀₀=0.5 was overlaid with 0.5%, 1%, and 1.5% (v/v) of *n*-hexadecane (Sigma). After vortexing for 1 min, the phases were permitted to separate for 15 min. Absorbance at 600 nm of the aqueous phase was then measured. The results were determined via this equation; $\{(A_0-A)/A_0\}\times 100$, where A_0 and A are, respectively, the initial and the final ODs of the aqueous phase.

Exopolysaccharide (EPS) isolation and analysis

Cells were grown in NB at 25°C, 220 rpm for 3 days. After centrifugation at 5,000 rpm for 20 min, the supernatant was collected. The EPSs were precipitated from culture supernatants with three volumes of cold ethanol and collected via 20 min of centrifugation at $12,000\times g$ at 4°C. The EPSs were air-dried, quantified, and normalized with cell dry mass.

Proteomic analysis and protein identification

Two-dimensional gel electrophoresis (2DE) was conducted by Genomine (<http://www.genomine.co.kr>). Duplicate gel electrophoresis confirmed the proteins with same location and intensity for identification processes. The samples were desalted using micro C18 ZipTips (Millipore), and the peptides were directly eluted with 5 mg/ml of CHCA in 60% ACN/0.1% TFA onto a MALDI plate. For the MS data, 200 shots were accumulated for each spectrum acquired from the Voyager-DE STR, and 1,000 shots from the TOF/TOF (Applied Biosystems, USA). All MS/MS data from the TOF/TOF was acquired using the default 1 kV MS/MS method. MS/MS data were primarily analyzed using the Proteomic Solution 1 system (Applied Biosystems), with Protein Prospector as the search engine.

Gene expression analysis by qRT-PCR

The cells were grown to mid-log phase (A_{600} of ~ 0.5) at 30°C in MSB medium containing either 10 mM sodium succinate or 1% (v/v) hexadecane as a sole carbon source. Total RNA was isolated from 3 ml of exponentially growing cells, using the RNeasy Mini kit (QIAGEN, USA), according to the manufacturer's instructions. cDNA was synthesized with 1 μ g RNA using primers of target genes and used as templates for quantitative real-time PCR (qRT-PCR) (Table 1). The PCR mixture contained 12.5 μ l of the iQ SYBR Green Supermix (Bio-Rad), 1 μ l of each primer (0.5 μ M) and 1.5 μ l of cDNA, which composed a total volume of 25 μ l. The PCR conditions were 95°C for 3 min, followed by 40 cycles of 45 sec at 95°C, 45 sec of 60°C, 45 sec of 72°C. To normalize the expression of each gene, expression level of 16S rDNA was quantified with the primers used by Watanabe *et al.* (2001). The quantification results were obtained from triplicate performance.

Results

Hexadecane degradation is hindered by sodium chloride and high temperature

In order to investigate the degradation of alkane by *Acinetobacter oleivorans* DR1, hexadecane degradation in MSB media was analyzed with a gas chromatograph equipped with a flame ionization detector (Fig. 1). After 96 h of monitoring, *Acinetobacter* sp. strain DR1 degraded 42% of hexadecane at 25°C and 30°C (Figs. 1A and B). This efficiency was not undermined by the presence of potassium chloride in media. However, when sodium chloride was added to media, only 22% and 19% of hexadecane were degraded at 25°C and 30°C,

Table 1. Primers used for quantitative real-time PCR

Gene	Function	Sequence (5'→3')	Size (bp)
AOLE_02800	Acyl-CoA dehydrogenase	TTCGGTGGTCATGGCTTTATTTCT TCATGGCAGCGTTGTCTTTATTTG	208
AOLE_07090	TonB-dependent siderophore receptor	TGACCACACCGCTTGAGTTTTTAG AATTTGGGCGTAGCTGTCTTCATA	269
AOLE_10740	Malate synthase G	TGAATGGCATCGCAACAATAA CTTTTTCAGCTCCGCCCTCTT	266
AOLE_14300	Isocitrate lyase	AAATCGACGGCTTCCAAACT TACGCGCAACGATGATACC	273
AOLE_17040	Putative ferric siderophore receptor protein	GCTCTTCTTCTGCCCTTGGTG TGTTCCGCGAGTTGCAGTATCTA	290
AOLE_17905	Multifunctional fatty acid oxidation complex subunit alpha	ATGGCGATGGCTGCTCCTAAA GGCTTGACCTGCTTGTAATGAAT	295

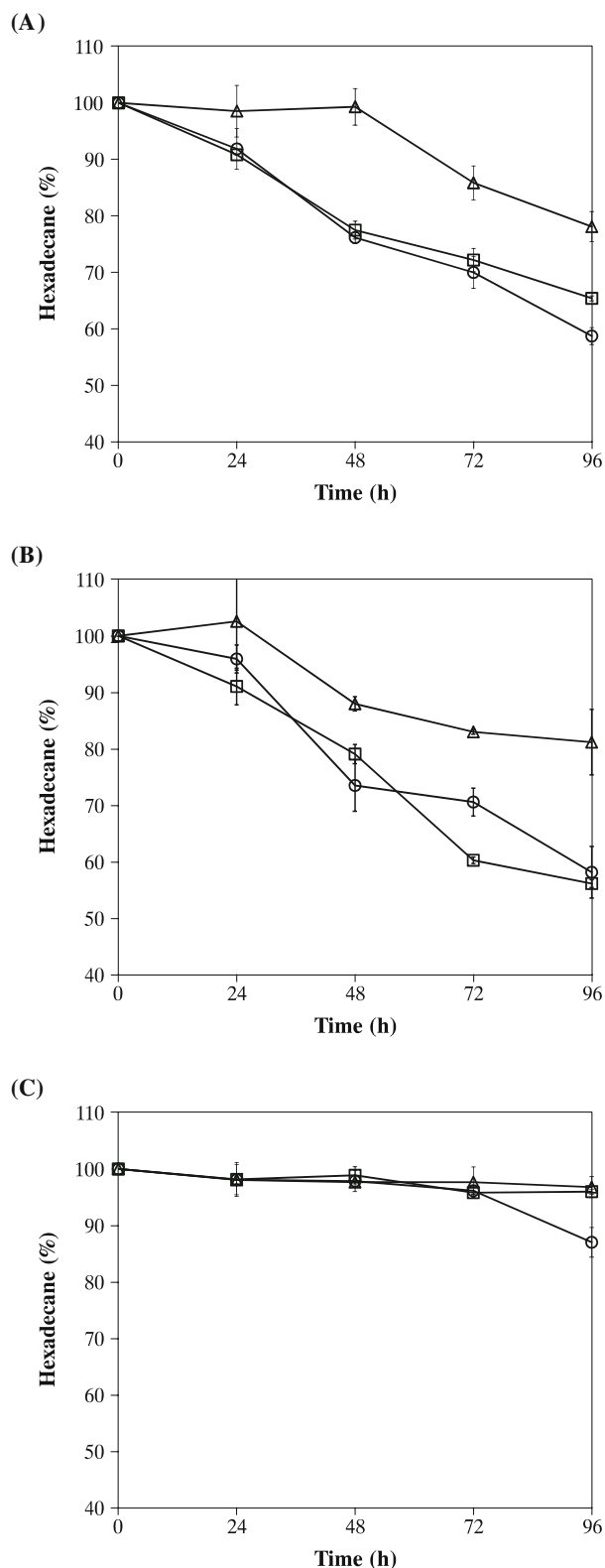


Fig. 1. Gas chromatographic analysis of hexadecane degradation at (A) 25°C, (B) 30°C, and (C) 37°C. Hexadecane degradation was inhibited by sodium chloride and high temperature (37°C). However potassium chloride did not affect hexadecane degradation. (○) MSB medium containing no salt; (△) MSB medium containing 1% NaCl; (□) MSB medium containing 1% KCl.

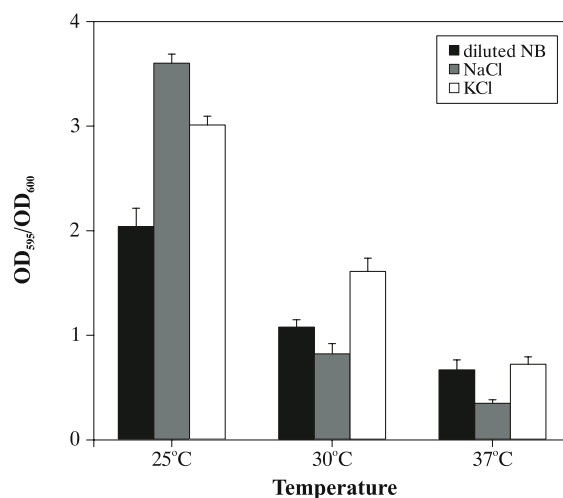


Fig. 2. Biofilm formation was tested in diluted nutrient broth, sodium chloride, or potassium chloride-added media. Biofilm formation was inhibited by sodium chloride at 30°C and 37°C whereas no inhibition was noted with potassium chloride. Lowering temperature promoted biofilm formation in all conditions. High temperature (37°C) reduced biofilm formation. Sodium chloride and high temperature are inhibitory factors of biofilm formation.

respectively. Only 13% of hexadecane was degraded at 37°C, thereby indicating that high temperatures were disadvantageous for hexadecane degradation by strain DR1 (Fig. 1C).

Inhibitory effect of sodium chloride and high temperature on biofilm formation

Biofilm formation on polystyrene surfaces was reduced to 76% and 52% when sodium chloride was added to the diluted NB at 30°C and 37°C, respectively (Fig. 2). This reduction did not recover for three days, implying that sodium chloride exerted an inhibitory effect on biofilm formation rather than retardation (data not shown). To the contrary, potassium chloride did not inhibit the biofilm formation of strain DR1. We did not observe the biofilm inhibition of sodium chloride at 25°C. Unlike at low temperature, only 62% of biofilm was formed at 37°C as compared with 30°C, in diluted NB. High temperature appears to be inhibitory to biofilm formation of strain DR1. The results of a variety of growth tests and viable cell counts confirmed that no growth defects occurred under such conditions. Taken together, sodium chloride and high temperature were identified as alkane degradation-inhibition factors. When biofilm formation was not successful because of high temperature and sodium chloride, hexadecane degradation was inefficient. Therefore, we concluded that biofilm formation was crucial to hexadecane degradation. To support the positive correlation between biofilm formation and hexadecane degradation, the use of a soluble compound, succinate, was evaluated. When cells were cultivated with succinate at 30°C and 37°C, CFU measured after 16 h of inoculation were $\sim 10^{12}$ CFU/ml regardless of temperature. However, when hexadecane was used as a sole carbon source, CFU was lower at 37°C (1.1×10^{15} CFU/ml at 30°C, 2.6×10^{11} CFU/ml at 37°C). This result shows that the extent of biofilm for-

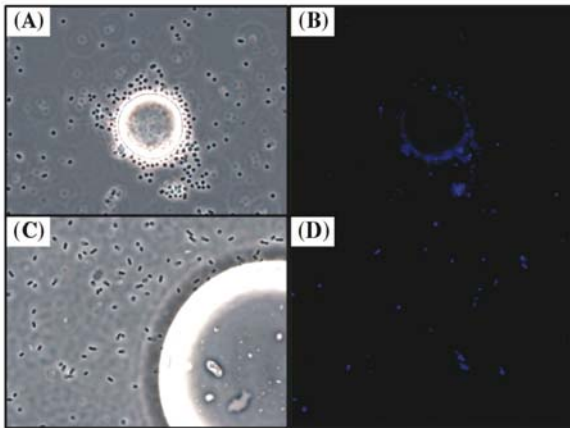


Fig. 3. Microscopy image shows that strain DR1 adheres to hexadecane droplet whereas *E. coli* GC4468 does not. (A) Strain DR1, phase-contrast; (B) strain DR1, DAPI staining; (C) GC4468, phase-contrast; (D) GC4468, DAPI staining.

mation is unrelated to the utilization of soluble compounds.

Effect of salts and temperatures on cell hydrophobicity

Cell hydrophobicity was changed in a negligible range by two salts at 25°C and 30°C as indicated by the MATH values ~40% and ~60%, respectively. Interestingly, the cells became hydrophobic when two salts were added to media at 37°C (MATH values 25%, diluted NB; 83%, NaCl; and 47%, KCl). Immediately after the MATH test, phase-contrast and fluorescent microscopic images of DAPI staining verified that strain DR1 attached to the interface of two phases and tended to aggregate with each other, forming a multilayer of cells on the hexadecane surface, whereas the *E. coli* strain GC4468 was neither attached nor aggregated with each other (Fig. 3). Collectively, no correlation was determined to exist between the MATH values and biofilm formation.

Mucoid phenotype of nonmotile cells and EPS production in the presence of salts

As shown in Fig. 4, *A. oleivorans* DR1 evidences swimming and swarming abilities on agar plates with a serrated edge on its swimming/swarming zone. Swimming motility was reduced by elevating temperature or adding sodium chloride and potassium chloride (Fig. 4A). Because there is no swimming motility at all in the presence of KCl, but hexadecane degradation was not affected under the same condition. We concluded that swimming motility is not related to hexadecane degradation. We determined the serrated edge of swarming zone as active motility. Active swarming motility was noted on NB agar at 25°C and 30°C (Fig. 4B). Our prolonged incubation confirmed the dispersion of swarming motility zone; therefore swarming at 25°C was active although the spreading zone looks smaller. It is worth noting that nonmotile cells on sodium chloride-added agar plates evidence a highly mucoid phenotype with round edges, whereas cells on potassium chloride-added agar plates were not significantly mucoid and maintained their serrated edges at temperatures of 25°C and 30°C. A positive correlation was noted to exist between

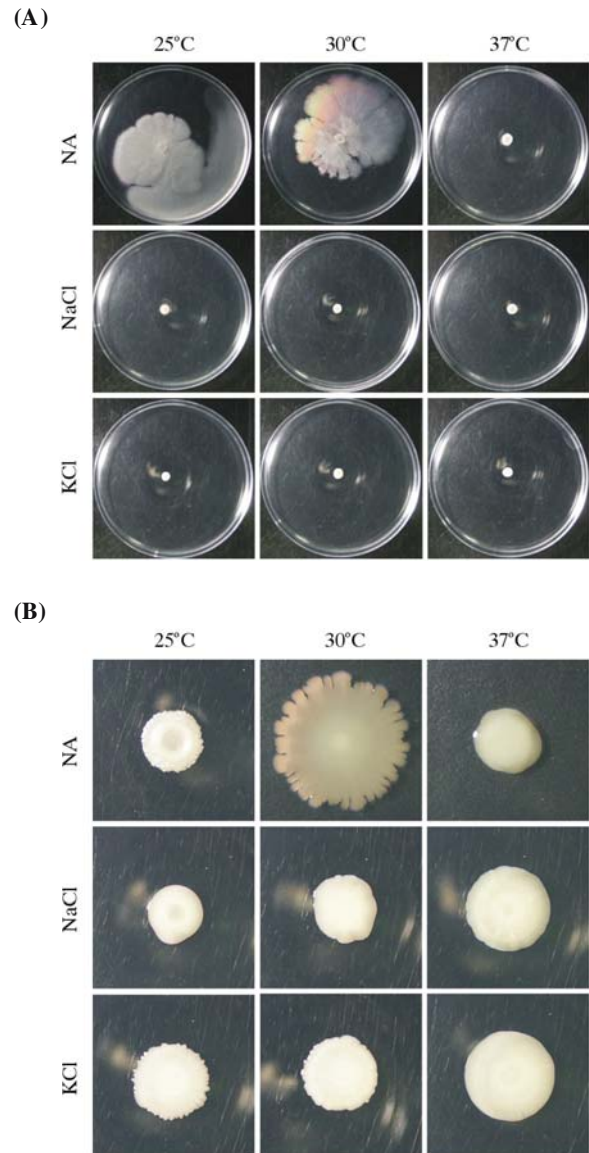


Fig. 4. Motility test. (A) Swimming, (B) Swarming. Swimming motility shown at 25°C and 30°C was inhibited via the addition of two ionic salts and high temperature (37°C). Swarming motility is inhibited by sodium chloride and high temperature. Non-swarming cells became mucous with round shape. Motility zone on potassium chloride-containing agar plate has serrated edge, which indicates active motility.

swarming motility and hexadecane degradation. Therefore, swarming motility may be a key factor in biofilm formation and hexadecane degradation. In order to confirm that there was no desiccation throughout experiments, swimming/swarming NB agar plates were transferred from 25°C and 37°C to 30°C and motility was restored in both. Because the mucoid phenotype is often found coupled with EPS overproduction, we attempted to determine whether two salts induce EPS overproduction in NB at 25°C. Strain DR1 produced EPS 0.24 ± 0.06 , 0.40 ± 0.04 and 0.55 ± 0.02 g/g in NB, sodium chloride and potassium chloride added NB, respectively. EPS overproduction in sodium chloride-added media was consistent with that de-

Table 2. Protein identification from 2DE

Spot no.	MW	pI	Protein	Differential abundance ^a
Peptide mass fingerprinting				
1611	52.2	4.4	Aspartyl/glutamyl-tRNA amidotransferase subunit B (GatB) [<i>Acinetobacter</i> sp. ADP1]	1.5
1618	56.1	5.1	Alkyl hydroperoxide reductase subunit F (AhpF) [<i>Acinetobacter</i> sp. ADP1]	2.7
1709	57.8	4.4	Chaperonin (GroEL) [<i>Acinetobacter</i> sp. ADP1]	4.5
2208	33.7	4.5	B12-dependent methionine synthase (MetH) [<i>Acinetobacter</i> sp. ADP1]	7.9
2303	41.0	4.6	Glycyl-tRNA synthetase subunit alpha (GlyQ) [<i>Acinetobacter</i> sp. ADP1]	1.9
2704	64.7	4.6	30S ribosomal protein S1 (RpsA) [<i>Acinetobacter</i> sp. ADP1]	2.6
2710	71.8	4.7	Polynucleotide phosphorylase/polyadenylase (PnpA) [<i>Acinetobacter</i> sp. ADP1]	3.2
2712	71.9	4.7	Polynucleotide phosphorylase/polyadenylase (PnpA) [<i>Acinetobacter</i> sp. ADP1]	45.4
2714	68.3	4.6	Phosphoenolpyruvate carboxykinase (Pck1) [<i>Acinetobacter</i> sp. ADP1]	3.7
2805	89.8	4.6	Bifunctional aconitate hydratase 2/2-methylisocitrate dehydratase (AcnB) [<i>Acinetobacter</i> sp. ADP1]	1.5
2806	110.3	4.6	Phosphoribosylformylglycinamide synthase (PurL) [<i>Acinetobacter</i> sp. ADP1]	3.2
2807	87.2	5.2	Phosphoenolpyruvate synthase (PpsA) [<i>Acinetobacter</i> sp. ADP1]	4.1
2808	80.2	4.7	Elongation factor G (FusA) [<i>Acinetobacter</i> sp. ADP1]	12.7
2809	84.8	4.7	Putative outer membrane protein (YP_046066) [<i>Acinetobacter</i> sp. ADP1]	2.1
2811	79.7	4.7	Elongation factor G (FusA) [<i>Acinetobacter</i> sp. ADP1]	2.6
2812	84.8	4.6	Putative outer membrane protein (YP_046066) [<i>Acinetobacter</i> sp. ADP1]	3.6
3703	59.2	4.8	Putative ABC transporter ATP-binding protein (YP_047866) [<i>Acinetobacter</i> sp. ADP1]	4.5
3809	103.1	4.8	Carbamoyl-phosphate synthase, large subunit (CarB) [<i>Acinetobacter</i> sp. ADP1]	6.6
3810	103.6	4.7	Carbamoyl-phosphate synthase, large subunit (CarB) [<i>Acinetobacter</i> sp. ADP1]	H
4801	86.7	4.9	Alanyl-tRNA synthetase (AlaS) [<i>Acinetobacter</i> sp. ADP1]	1.9
5711	62.4	5.2	Acyl-CoA dehydrogenase B (AcdB) [<i>Acinetobacter</i> sp. M-1]	H
5802	80.7	5.2	Malate synthase G (GlcB) [<i>Acinetobacter</i> sp. ADP1]	5.3
5805	80.1	5.1	Malate synthase G (GlcB) [<i>Acinetobacter</i> sp. ADP1]	156.5
6612	55.2	5.4	Isocitrate lyase (AceA) [<i>Acinetobacter</i> sp. ADP1]	12.1
7701	57.3	5.5	Ubiquinone oxidoreductase (EtfD) [<i>Acinetobacter</i> sp. SE19]	3.4
8511	48.1	6.4	NADH dehydrogenase I chain F (NuoF) [<i>Acinetobacter</i> sp. ADP1]	6.1
MS/MS sequencing				
2402	51.9	4.4	Phosphopyruvate hydratase (Eno, AOLE_08350)	4.3
3505	57.4	4.6	ATP synthase subunit beta (AOLE_18565)	3.1
5104	35.4	5.0	2,3,4,5-tetrahydropyridine-2,6-carboxylate N-succinyltransferase (DapD, AOLE_04475)	2.1
3801	79.2	4.7	bifunctional aconitate hydratase 2/2-methylisocitrate dehydratase (AOLE_06510)	2.0
5309	48.3	5.0	S-adenosylmethionine synthetase (AOLE_11050)	2.6
5501	58.7	4.9	ATP synthase subunit alpha (AOLE_18575)	2.0
5504	59.7	4.9	Argininosuccinate synthase (AOLE_14010)	3.7
6209	44.5	5.3	UDP-glucose 4-epimerase (AOLE_19055)	3.2
6301	48.3	5.1	S-adenosylmethionine synthetase (AOLE_11050)	4.2
6312	46.5	5.2	NAD(P) transhydrogenase subunit alpha (AOLE_16625)	4.1
6411	50.3	5.3	Aspartate aminotransferase A (AOLE_04615)	2.4
6502	59.9	5.1	Fumarate hydratase (AOLE_17010)	5.8
6702	73.5	5.3	Acyl-CoA dehydrogenase (AOLE_02800)	H
6703	87.0	5.3	TonB-dependent siderophore receptor (AOLE_07090)	H
6809	100.7	5.2	Malate synthase G (AOLE_10740)	H
7006	25.4	5.5	Superoxide dismutase (AOLE_05305)	2.1
7010	16.1	5.5	50S ribosomal protein L10 (RplJ, AOLE_18010)	2.1
7107	30.1	5.4	Hypothetical protein (AOLE_03815)	9.8
7210	41.5	5.6	Succinyl-CoA synthetase subunit alpha (AOLE_03735)	2.8
7310	48.1	5.6	Putative alcohol dehydrogenase (AOLE_06670)	3.5
7312	48.6	5.6	Putative alcohol dehydrogenase (AOLE_06670)	2.4
7407	51.8	5.6	Putative alcohol dehydrogenase (AOLE_06670)	2.2
7611	71.7	5.6	Electron transfer flavoprotein-ubiquinone oxidoreductase (AOLE_17540)	4.5
7805	99.8	5.6	Putative ferric siderophore receptor protein (AOLE_17040)	H
8004	17.2	5.7	Acetolactate synthase 3 regulatory subunit (IlvH, AOLE_16715)	3.3

Table 2. Continued

Spot no.	MW	pI	Protein	Differential abundance ^a
8304	47.7	5.8	Alcohol dehydrogenase, class IV (AOLE_03630)	4.1
8308	47.6	6.2	Alcohol dehydrogenase, class IV (AOLE_03630)	24.8
8312	48.3	6.4	Acetyl-CoA acetyltransferase (AOLE_03005)	7.4
8313	46.0	6.8	3-Ketoacyl-CoA thiolase (FadA, AOLE_17910)	12.7
8405	51.5	6.0	Glutamate dehydrogenase (AOLE_14205)	3.1
8711	86.7	6.6	Multifunctional fatty acid oxidation complex subunit alpha (FadB, AOLE_17905)	H
9202	42.8	7.5	Branched-chain amino acid aminotransferase (AOLE_02705)	3.6
9301	48.2	7.3	D-3-Phosphoglycerate dehydrogenase (AOLE_01695)	3.3
9402	52.3	7.1	Diaminobutyrate-2-oxoglutarate aminotransferase (AOLE_04880)	2.2
9601	68.1	7.6	Acetolactate synthase 3 catalytic subunit (AOLE_16720)	5.4

Strain DR1 was grown in MSB media with 1% hexadecane or 10 mM sodium succinate as a sole carbon source at 30°C. Cells were harvested at OD₆₀₀ ~ 0.7. Proteins were identified by either peptide mass fingerprinting or MS/MS sequencing.

^a Listed proteins were expressed in cells grown in hexadecane by designated fold. 'H' means the proteins exclusively detected from hexadecane grown-cells.

^b AOLE is the locus tag of *Acinetobacter oleivorans* DR1 genome (GenBank accession no. CP002080).

scribed in our previous report (Kang and Park, 2010a). Collectively, our results show that the mucoid phenotype can be associated with sodium chloride-induced EPS, significantly affecting biofilm formation and hexadecane degradation.

Changes in carbon fluxes and stress responses identified in proteomic analysis

Differentially expressed 195 spots were detected via 2DE. Initially, we attempted to identify 65 spots that were upregulated by more than 3-fold in hexadecane-grown cells. Because only 26 proteins were identified by peptide mass fingerprinting, we conducted a MALDI-TOF MS/MS method that targeted additional 35 proteins. Finally, a total of 61 proteins were identified (Table 2). The genome of strain DR1 has been completed because of its biotechnological potential (Jung and Park, 2010). Protein sequences from proteomic approach were searched in the whole genome sequence of strain DR1 (GenBank database CP002080). Upregulated fatty acid me-

tabolism was identified (FadA, 3-Ketoacyl-CoA thiolase; FadB, Multifunctional fatty acid oxidation complex subunit alpha; and AcdB, Acyl-CoA dehydrogenase B). This is because the terminal oxidation of alkane produces alkanol, which is subsequently oxidized by beta-oxidation. The glyoxylate pathway and gluconeogenesis were also upregulated (AceA, Isocitrate lyase; GlcB, Malate synthase G; PpsA, Phosphoenolpyruvate synthase), because bacterial cells need to synthesize all cellular precursors from hexadecane at a rapid rate. Upregulated expression of several genes was also confirmed by qRT-PCR method (Fig. 5). The level of those expressions is ranged from 5.2 to 10.6-folds except tonB-dependent siderophore receptor (AOLE_07090). Expression of the AOLE_07090 may not be regulated at transcriptional level. However, this discrepancy remains to be elucidated. Interestingly, several stress response-related proteins were up-regulated (AhpF, Alkyl hydroperoxide reductase subunit F; AOLE_05305, Superoxide dismutase; GroEL, Chaperonin). This may be attributable to unavoidable oxidative stress, because alkane metabolism is a continuous oxidation process that includes the terminal oxidation of alkane and the beta-oxidation of fatty acid. Therefore, bacterial cells have to reorganize their stress defense mechanisms, as well as their metabolic pathways, to utilize alkane.

Discussion

According to the results of our previous study (Kang and Park, 2010a), sodium chloride, hexadecane, and diesel fuel induce EPS production in *A. oleivorans* DR1, and sodium chloride-induced EPS evidences a protective effect against diesel toxicity. Based on the results of this study, sodium chloride should inhibit the formation of biofilms on diesel fuel via the overproduction of EPS. Because the strategy by which the cells overcome low solubility of hydrocarbon is blocked, the accessibility to diesel fuel is subsequently compromised. We speculate that inefficient access to diesel fuel delays toxic activity on cells, and thus cells can have time to sense and adapt to stress via the alteration of physiologies and metabolisms. Although the utilization of carbon sources is delayed, this can be rewarded by a guaranteed higher survival rate.

Motility has been reported rarely in *Acinetobacter* spp. and

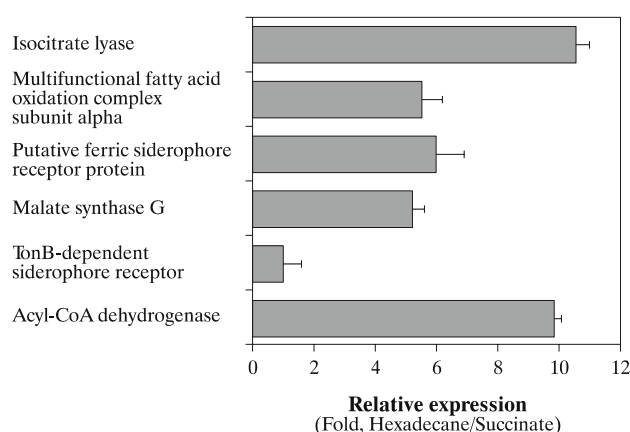


Fig. 5. Expression of genes was assessed at the transcriptional level when different compounds (hexadecane, succinate) were utilized as a sole carbon source. Selected genes encode proteins that are exclusively expressed in cells utilizing hexadecane as a carbon source except isocitrate lyase (Table 2.). Gene expression level in cells growing on hexadecane was compared with the value of cells growing on succinate.

is considered a feature of this genus (Bergogne-Berezin and Towner, 1996). Hence, the observed motility of the DR1 strain is a very interesting feature. Moreover, the recent genome sequencing data of several *Acinetobacter* spp. identified the genomic regions involved in cellular appendages such as type IV pili, flagella, and fimbriae (Vallenet *et al.*, 2008; Jung and Park, 2010), indicating that other *Acinetobacter* spp. would evidence motility. Mucoid colonies of non-motile cells were frequently observed to be coupled with EPS production in several bacteria, including *Vibrio cholerae* (Ali *et al.*, 2000). Consistent with our previous report (Kang and Park, 2010a), colonies of strain DR1 became mucoid when they were non-motile on sodium chloride-added agar plates. However, potassium chloride did not affect colony morphology and swarming motility, despite the overproduction of EPS. Different regulation of EPS production, motility, and colony shape by two ionic salts might affect biofilm formation and the degradation of hexadecane. Among tested phenotypes, swarming motility was identified as a key phenotypic factor with a positive correlation in biofilm formation and hexadecane degradation. This close relationship between motility and biofilm formation has been reported previously. The cells were held together by pili-like structures in the biofilm matrix of *Acinetobacter baumannii* 19606 according to electron microscopic analyses, although motility was not noted under the tested conditions (Tomaras *et al.*, 2003). Additionally, the non-adherent mutant of *Acinetobacter calcoaceticus* RAG-1, MR-481 lacking thin fimbriae, proved unsuccessful in terms of its ability to adhere to polystyrene and hexadecane (Rosenberg *et al.*, 1982). MR-481, which is incapable of adhering, failed to grow on hexadecane, and the revertant of this mutant regained the ability to adhere to and grow on hexadecane.

Sodium chloride exerts an inhibitory effect on biofilm formation and hexadecane degradation in strain DR1, whereas potassium chloride does not, thereby implying that the EPS induced by each salt plays a different role. This difference may result from the composition of EPS. The composition and amount of EPS synthesized by cells vary with nutritional condition (Onbasli and Aslim, 2009). The physicochemical properties of EPS may affect bacterial adhesion to surfaces and biofilm maturation. In terms of the electrostatic charge of EPS, the majority is polyanionic, but some are neutral and a very few are polycationic (Sutherland, 2001). Ion-regulated EPS production has been previously reported in several bacteria. Among related reports, most importantly, EPS overproduction was an adaptive mechanism in response to osmotic stress in the *E. coli* K-12 *rpoS* mutant. Defects in EPS overproduction and colonic acid biosynthesis were shown to limit growth in a saline medium. As *rpoS* is crucial for stress responses, EPS overexpression has been strongly suggested as an alternative response in this mutant strain (Ionescu and Belkin, 2009). Similarly, *Acinetobacter* sp. strain DR1 may overproduce EPS in response to osmotic stress.

Proteomic analysis identified the intracellular modulation of metabolic pathways. Because hexadecane was used as a sole carbon source, terminal oxidation of alkane followed by beta-oxidation is the only carbon assimilation pathway, and related proteins such as acyl-CoA dehydrogenase, 3-ketoacyl-CoA thiolase, and 3-hydroxyacyl-CoA dehydrogenase were upregulated in hexadecane-grown cells. Upregulation of the

glyoxylate pathway was also identified. According to another proteomic study, the upregulated glyoxylate pathway might prove to be a shortcut for providing cellular precursors from one available carbon source and avoiding the release of carbon dioxide (Sabirova *et al.*, 2006). The induction of alkyl hydroperoxide reductase, which is responsible for reducing organic hydroperoxides, indicates that the DR1 strain modulates its defense mechanism to cope with oxidative stress originating from the continuous oxidation of the alkane chain. Subsequent DNA damage is highly anticipated according to the upregulation of DNA repair-related proteins.

In conclusion, we have demonstrated herein that *A. oleivorans* DR1 modulates physiologies and metabolisms for efficient hexadecane utilization. To the best of our knowledge, this is the first report in which the quantitative correlation between biofilm formation and alkane degradation has been described, even though the importance of biofilms in hydrocarbon utilization has been previously suggested. Additionally, proteomic analysis indicated that successful defenses against the stress caused during alkane degradation should be considered for use in the bacterial bioremediation of alkanes.

Acknowledgements

This work was supported by a grant from the MEST/NRF program (grant #: 2010-0076488), Republic of Korea, to W.P.

References

- Ali, A., J.A. Johnson, A.A. Franco, D.J. Metzger, T.D. Connell, J.G. Morris, and S. Sozhamannan. 2000. Mutations in the extracellular protein secretion pathway genes (*eps*) interfere with rugose polysaccharide production in and motility of *Vibrio cholera*. *Infect. Immun.* 68, 1967-1974.
- Baldi, F., N. Ivošević, A. Minacci, M. Pepi, R. Fani, V. Svetlicic, and V. Zutić. 1999. Adhesion of *Acinetobacter venetianus* to diesel fuel droplets studied with in situ electrochemical and molecular probes. *Appl. Environ. Microbiol.* 65, 2041-2048.
- Bergogne-Berezin, E. and K.J. Towner. 1996. *Acinetobacter* spp. as nosocomial pathogens: microbiological, clinical, and epidemiological features. *Clin. Microbiol. Rev.* 9, 148-165.
- Ionescu, M. and S. Belkin. 2009. Overproduction of exopolysaccharides by an *Escherichia coli* K-12 *rpoS* mutant in response to osmotic stress. *Appl. Environ. Microbiol.* 75, 483-492.
- Jung, J. and W. Park. 2010. Complete genome sequence of the diesel-degrading *Acinetobacter* sp. strain DR1. *J. Bacteriol.* 192, 4794-4795.
- Kang, Y.S., J. Jung, C.O. Jeon, and W. Park. 2010. *Acinetobacter oleivorans* sp. nov. is capable of adhering to and growing on diesel-oil. *J. Microbiol.* In Press
- Kang, Y.S. and W. Park. 2010a. Protection against diesel oil toxicity by sodium chloride-induced exopolysaccharides in *Acinetobacter* sp. strain DR1. *J. Biosci. Bioeng.* 109, 118-123.
- Kang, Y.S. and W. Park. 2010b. Contribution of quorum-sensing system to hexadecane degradation and biofilm formation in *Acinetobacter* sp. strain DR1. *J. Appl. Microbiol.* 109, 1650-1659.
- Kang, Y.S. and W. Park. 2010c. Trade-off between antibiotic resistance and biological fitness in *Acinetobacter* sp. strain DR1. *Environ. Microbiol.* 12, 1304-1318.
- Lee, Y., Y. Kim, S. Yeom, S. Kim, S. Park, C.O. Jeon, and W. Park. 2008. The role of disulfide bond isomerase A (DsbA) of *Escherichia coli* O157: H7 in biofilm formation and virulence. *FEMS Microbiol. Lett.* 278, 213-222.
- Onbasli, D. and B. Aslim. 2009. Effects of some organic pollutants on the exopolysaccharides (EPSs) produced by some *Pseudomonas*

- spp. strains. *J. Hazard Mater.* 168, 64-67.
- O'Toole, G.A. and R. Kolter. 2006. Flagellar and twitching motility are necessary for *Pseudomonas aeruginosa* biofilm development. *Mol. Microbiol.* 30, 295-304.
- Pompilio, A., R. Piccolomini, C. Picciani, D. D'Antonio, V. Savini, and G. Di Bonaventura. 2008. Factors associated with adherence to and biofilm formation on polystyrene by *Stenotrophomonas maltophilia*: the role of cell surface hydrophobicity and motility. *FEMS Microbiol. Lett.* 287, 41-47.
- Rosenberg, M., E.A. Bayer, J. Delarea, and E. Rosenberg. 1982. Role of thin fimbriae in adherence and growth of *Acinetobacter calcoaceticus* RAG-1 on hexadecane. *Appl. Environ. Microbiol.* 44, 929-937.
- Rosenberg, M., D. Gutnick, and E. Rosenberg. 1980. Adherence of bacteria to hydrocarbons: a simple method for measuring cell-surface hydrophobicity. *FEMS Microbiol. Lett.* 9, 29-33.
- Sabirova, J.S., M. Ferrer, D. Regenhardt, K.N. Timmis, and P.N. Golyshin. 2006. Proteomic insights into metabolic adaptations in *Alcanivorax borkumensis* induced by alkane utilization. *J. Bacteriol.* 188, 3763-3773.
- Schneiker, S., V.A.P. Martin dos Santos, D. Bartels, T. Bekel, M. Brecht, J. Buhrmester, T.N. Chernikova, and *et al.* 2006. Genome sequence of the ubiquitous hydrocarbon-degrading marine bacterium *Alcanivorax borkumensis*. *Nat. Biotechnol.* 24, 997-1004.
- Stanier, R.Y., N.J. Palleroni, and M. Doudoroff. 1966. The aerobic pseudomonads: a taxonomic study. *J. Gen. Microbiol.* 43, 159-271.
- Sutherland, I. 2001. The biofilm matrix an immobilized but dynamic microbial environment. *Trends Microbiol.* 9, 222-227.
- Tomaras, A.P., C.W. Dorsey, R.E. Edelmann, and L.A. Actis. 2003. Attachment to and biofilm formation on abiotic surfaces by *Acinetobacter baumannii*: involvement of a novel chaperone-usher pili assembly system. *Microbiology* 149, 3473-3484.
- Vallenet, D., P. Nordmann, V. Barbe, L. Poiriel, S. Mangenot, E. Bataille, C. Dossat, and *et al.* 2008. Comparative analysis of Acinetobacters: three genomes for three lifestyles. *PLoS One* 3, e1805.
- van Loosdrecht, M.C., W. Norde, and A.J. Zehnder. 1990. Physical chemical description of bacterial adhesion. *J. Biomater. Appl.* 5, 91-106.
- Watanabe, K., Y. Kodama, and S. Harayama. 2001. Design and evaluation of PCR primers to amplify bacterial 16S ribosomal DNA fragments used for community fingerprinting. *J. Microbiol. Methods* 44, 253-262.